RSC Advances

PAPER

View Article Online
View Journal | View Issue

Cite this: *RSC Adv.*, 2018, **8**, 26377

In situ growth of ZIF-67 on a nickel foam as a three-dimensional heterogeneous catalyst for peroxymonosulfate activation

Lin Peng,[a] Xiaobo Gong,*[ab] Xinghong Wang,[a] Zhao Yang[a] and Yong Liu[ab]

Received 12th June 2018
Accepted 11th July 2018

DOI: 10.1039/c8ra05024d

rsc.li/rsc-advances

Advanced oxidation processes based on sulfate radicals have been widely used to eliminate contaminants. In this study, an efficient cobalt-based three-dimensional heterogeneous catalyst was fabricated through *in situ* growth of ZIF-67 on nickel foam (NF/ZIF-67). The factors influencing NF/ZIF-67-activated peroxymonosulfate (PMS) were investigated. Enhanced RhB degradation was observed using NF/ZIF-67-activated PMS under neutral conditions and high temperatures. Sulfate radicals were the dominant active species for the oxidative decolorization of RhB with NF/ZIF-67-activated PMS. NF/ZIF-67 was easily separated from the solution, and it also retained high catalytic stability. This study provides a rapid and mild method for the fabrication of promising three-dimensional heterogeneous catalysts for PMS activation and wastewater treatment.

Introduction

In recent years, advanced oxidation processes (AOPs) based on sulfate radicals have drawn widespread attention because of their potential capability in the treatment of bio-recalcitrant organic compounds in wastewater.[1–4] Sulfate radicals, which can be produced by the activation of peroxymonosulfate (PMS), show high oxidation activity owing to high redox potential of 2.5–3.1 V and longer half-life period (30–40 μs) than that of ·OH (20 ns).[5,6] UV irradiation, heating, and ultrasound have been developed for activating peroxymonosulfate[7] and require high energy input when they are used for wastewater treatment. Recently, transition metal-based materials such as Fe^{2+} and Co^{2+} have been considered as efficient catalysts for PMS activation.[8–11] However, the utilization of homogeneous metal ions to activate PMS leads to catalyst loss and possible secondary contamination. Furthermore, homogenous catalysts are very difficult to recycle and separate from the solution. At various pH conditions, transition metal ions form different species. In alkaline conditions, the transition metal ions transform into hydroxide precipitates. In acidic conditions, they form hydrates. The change in species might reduce the catalyst availability for activating PMS. Thus, catalysts based on heterogeneous transition metals are desired for activating PMS. Until now, cobalt-SBA-15 and other heterogeneous catalysts based on transition metals have been applied for PMS activation and sulfate radical generation.[12–14] The structure, size distribution, and morphology of transition metal catalysts determine their performance for PMS activation. For practical purposes, these heterogeneous catalysts were further developed through coordination with ligands or by loading on carriers to increase the active surface area and enhance the catalyst stability.

Metal–organic frameworks (MOFs), which are composed of organic–inorganic crystals,[15,16] have been explored and have shown potentials for many applications such as gas storage and separation, catalysis, and sensors.[17–19] In addition, MOFs have become widespread in environmental applications, such as the adsorption and degradation of organic pollutants, due to their unique structures, large surface areas, and abundant active sites.[20–22] MOFs, bearing transition metal species and doped-nitrogen species, can be used as alternative catalysts for activating oxidants and generating free radicals. ZIF-8-derived porous carbon displays the best performance in the degradation of phenol by both ·OH and $SO_4^{\cdot-}$ through PMS activation.[23] The transition metal cobalt has been widely investigated and has proven to be an effective activator of PMS. Thereby, ZIF-67, which is a cobalt-based MOF, has been explored as a heterogeneous catalyst for PMS activation with high catalytic activity and good stability in the degradation of dyes.[24] The Co_3O_4 nanospheres derived from ZIF-67 with a 3D-nano structure can effectively activate PMS to degrade dyes with a rate constant of 0.0509 min^{-1} under neutral conditions.[25]

However, MOFs and MOF-based catalysts are typically obtained as fine powders, which are difficult to separate from solutions. Moreover, the fine powders must be processed to form blocks for realistic large-scale operations, which require special equipment and complex processes. Thus, porous structures such as silica foams, ceramic foams, and polysulfone

[a]*College of Chemistry and Materials Science, Sichuan Normal University, Chengdu, Sichuan 610066, China. E-mail: gxb@sicnu.edu.cn; Fax: +86-028-84760802; Tel: +86-028-84760802*

[b]*Key Laboratory of Special Waste Water Treatment, Sichuan Province Higher Education System, Chengdu, Sichuan 610066, China*

have been explored as supports to develop large-scale heterogeneous catalysts having the properties of micro/nanoporous structure-based nanoscale materials and macroporous structures from the supports.[26,27] Usually, the vast majority of large-scale heterogeneous catalysts are fabricated through hydrothermal methods and similar approaches, which require toxic solvents and long preparation times.[27] Therefore, it remains essential and significant to rapidly and mildly fabricate catalysts into large-sized 3D materials for PMS activation.

Hence, a cobalt-based metal–organic framework, *i.e.*, the zeolitic imidazolate framework (ZIF)-67 was grown *in situ* on commercial nickel foam (NF) for the efficient activation of peroxymonosulfate and degradation of rhodamine B (RhB). The catalytic activity of NF/ZIF-67 was evaluated for the catalytic oxidation of RhB by the activation of PMS in an aqueous solution. On the basis of the unique and porous structure and abundant active sites, the as-prepared three-dimensional heterogeneous catalysts exhibited high PMS activation efficiency and good stability.

Results and discussion

Characterizations of NF/ZIF-67

The morphology and structure of pure NF and NF/ZIF-67 were characterized by scanning electron microscopy (SEM). As can be seen from Fig. 1A, the original nickel foam had a relatively smooth surface without any impurities. The diameter of the NF backbone was around 40 μm. After growing for 12 h, the surface of NF was no longer smooth but rough and presented numerous particles (Fig. 1B and inset). In the enlarged image of NF/ZIF-67, the surface of NF was covered with a layer of ZIF-67. The ZIF-67 grown on NF had an average size of 1.0 μm. After the catalytic reaction (Fig. 1C and inset), ZIF-67 on NF almost lost its initial morphology. Nevertheless, the collapsed ZIF-67 covered the NF skeleton, and it could still act as a catalyst for PMS activation to degrade rhodamine B. EDX (Fig. 1D and inset) shows that the elemental composition of NF/ZIF-67 included Ni, Co, C, N and O. The cobalt atoms in ZIF-67 on the surface of NF could act as catalyst centres for the activation of PMS during AOPs. The results indicated that ZIF-67 was successfully grown *in situ* on the nickel foam with uniform distribution on the backbones. The three-dimensional heterogeneous structure might be beneficial for the transfer of reactants and reaction products.

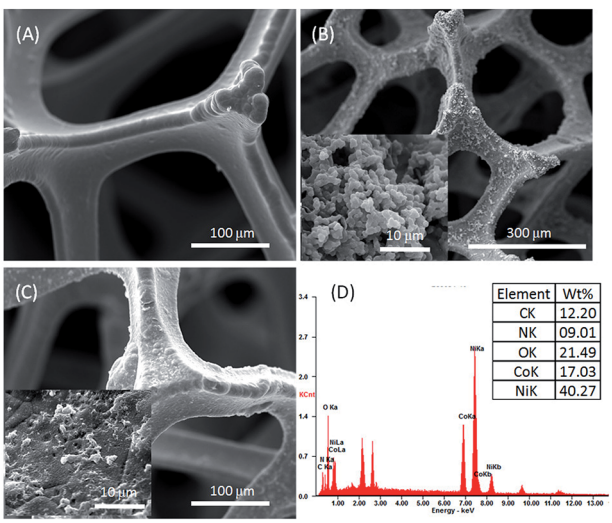

Fig. 1 SEM images of (A) pure NF, NF/ZIF-67 (B) before and (C) after the catalytic process, and (D) EDX spectrum of NF-ZIF-67. The insets of (B) and (C) are the enlarged SEM images. The inset of (D) is the element content based on the EDX data.

Catalytic performance of RhB degradation

To explore the catalytic activity of NF/ZIF-67 in detail, rhodamine B was selected as a model contaminant. Fig. 2 reveals the removal efficiencies under different catalysts with or without PMS. When only NF, ZIF-67 and NF/ZIF-67 were present in the solution without PMS, negligible amounts of RhB were removed *via* adsorption after 30 min, demonstrating that NF, ZIF-67 and NF/ZIF-67 have weak affinities for RhB adsorption, thus, adsorption contributed less to the decolorization of RhB. Meanwhile, the decolorization of RhB with only PMS was also carried out to confirm the role of NF/ZIF-67 in the activation of PMS. It was found that RhB was slightly degraded with only 5% removal efficiency due to the weak oxidation activity of SO_5^{2-}.[2,3] Pure NF with PMS had no catalytic activity on the decolorization of RhB except for slight adsorption. Clearly, with ZIF-67 grown *in situ* on NF, more than 99% of RhB was removed in 30 min with PMS and NF/ZIF-67, indicating that NF/ZIF-67 was highly active towards PMS activation to generate sulfate radicals and/or hydroxyl radicals to decolorize RhB in water. The rate constant (k) of NF/ZIF-67 was 0.285 min^{-1}, which was slower than that of ZIF-67 (0.391 min^{-1}) alone with a dosage of 25 mg L^{-1}.[24] However, NF/ZIF-67 still maintained relatively high activity. Notably, NF/ZIF-67 could be easily separated from the solution. Only about 0.46 mg L^{-1} of cobalt ions was dissolved in the solution of the NF/ZIF-67 catalyst during 30 min of degradation at 25 °C. The dissolved amounts of cobalt ions appeared to be insufficient for PMS activation in aqueous solution.

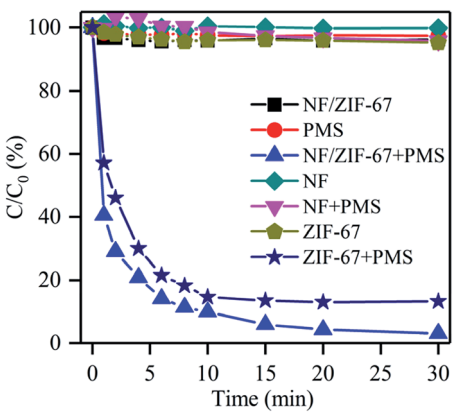

Fig. 2 Degradation of RhB with different catalysts with or without PMS. Reaction conditions: initial pH of 7.0, initial RhB concentration of 100 mg L^{-1}, PMS dosage of 30 mg, and temperature of 25 °C.

Effects of NF/ZIF-67-activated PMS on RhB degradation

The role of PMS dosage on RhB decolorization in the system with the NF/ZIF-67 catalyst is shown in Fig. 3A. The removal efficiencies of RhB with PMS dosages of 20 mg, 30 mg and 40 mg after 30 min operation were 78.3%, 97.0% and 99.5%, respectively. As a result, the increased dosage of PMS enhanced the decolorization kinetics. The k value of RhB degradation also increased from 0.169 min^{-1} to 0.556 min^{-1}. Owing to fewer sulfate radicals in the system, lower RhB degradation was obtained due to less PMS dosage. It is noted that only 2.5% of RhB in the solution could be decolorized by PMS alone, as shown in Fig. 2. These results further indicated that NF/ZIF-67 possessed excellent ability for activating PMS to produce free radicals for RhB degradation. Fig. 3B displays the effect of initial RhB concentration on decolorization by the AOP system; it demonstrates that higher RhB concentration leads to lower degradation of RhB, which could be due to large amounts of intermediates generated in the high-RhB-concentration solution adsorbed on the surface of ZIF-67, thus impeding the close contact interface between the active sites of NF/ZIF-67 and PMS.[28]

The pH of a solution might affect transitional metal species formation and their availability to react with the oxidant, indicating that the pH of the solution plays a key role in oxidant decomposition and free radical generation. As shown in Fig. 3C, the removal efficiency increased from 89.0% to 97.0% as the initial pH of the solution increased from 3.0 to 7.0, revealing that neutral conditions favour RhB degradation by NF/ZIF-67 compared to acidic conditions. The rate constant of RhB degradation increased from 0.132 min^{-1} to 0.285 min^{-1}. The surface of ZIF-67 was positively charged, and the cationic dye of RhB was also positively charged.[29] The carboxylic group of RhB could dissociate to $-COO^-$ in acidic conditions. Under acidic conditions, the positive charge of ZIF-67 increased the electrostatic repulsion between the negatively charged part of RhB and the anionic sulfate radicals, resulting in less contact between NF/ZIF-67 and RhB. In addition, pH may affect the reactivity between ZIF-67 and PMS on the catalyst surface as well as that between RhB and sulfate radicals in the bulk solution, hindering RhB degradation. On the other hand, the relatively high stability of PMS was less conducive to the activation process under acidic conditions.[3] It is worth mentioning that the RhB removal efficiency and the rate constant significantly decreased to 75.0% and 0.084 min^{-1}, respectively, when the initial pH was further increased to 9.0. The results indicated that basic conditions do not favour the degradation of RhB by NF/ZIF-67-activated PMS; this may be due to the self-decomposition of PMS under basic conditions and the decrease in the effective PMS amount, which lead to low degradation efficiency.[30,31] Moreover, the increase in pH increased the amount of negative surface charges of the activator due to the accumulation of OH^- under basic conditions. At the same time, the proportion of SO_5^{2-} decreased, hindering the static interactions between the surface of NF/ZIF-67 and the PMS species, which led to the decrease in the extent and kinetics of degradation.[32]

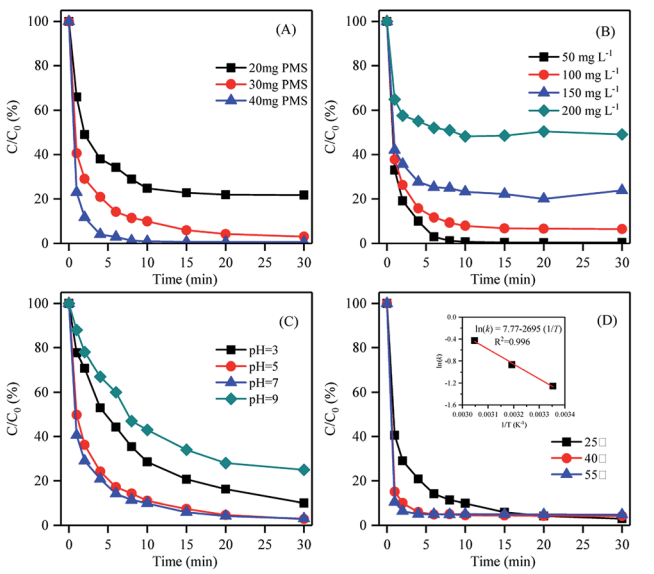

Fig. 3 Effects of (A) PMS dosage, (B) initial RhB concentration, (C) initial pH, and (D) temperature on the degradation of RhB with NF/ZIF-67-activated PMS.

The catalytic degradation of RhB by NF/ZIF-67 at different temperatures has also been explored (Fig. 3D). The reaction temperature exhibited a small effect on RhB degradation. A weak temperature dependence of the catalytic activity was observed in the system, highlighting the inherent excellent catalytic performance of NF/ZIF-67. However, the decolorization kinetics remarkably enhanced from 0.285 min^{-1} to 0.420 min^{-1} when the temperature increased from 25 °C to 40 °C. When the temperature was further increased to 55 °C, the rate constant increased to 0.652 min^{-1}, and the time for complete removal of RhB was shortened to only 4 min, indicating that temperature plays an important role in activating PMS and RhB degradation. As higher temperature leads to faster rate constants, an Arrhenius equation between the temperature and rate constant was established to calculate the activation energy of RhB degradation. As shown in the inset of Fig. 3D, good linear regression ($R^2 = 0.996$) demonstrated that the reaction kinetics of RhB degradation by the NF/ZIF-67/PMS system could be suitably correlated with temperature *via* the Arrhenius equation. The activation energy for the decolorization of RhB was calculated to be 22.4 kJ mol^{-1}, which was lower than that reported previously,[11,33,34] indicating that higher catalytic activation of PMS was achieved on NF/ZIF-67.

Possible mechanism of PMS activation

The above-mentioned results indicated that the addition of PMS to the as-prepared NF/ZIF-67 heterogeneous catalyst could degrade RhB effectively. However, the addition of only NF, ZIF-67 or NF/ZIF-67 had negligible effects on the decolorizationn of RhB. Moreover, NF with PMS also exhibited less efficiency for the decolorization of RhB. Thus, it was speculated that the *in situ* growth of ZIF-67 on nickel foam could accelerate PMS activation and generate abundant sulfate and hydroxyl radicals for RhB degradation. As mentioned in literature, the cobalt ions

in NF/ZIF-67 can interconvert between Co^{2+} and Co^{3+} when they are adsorbed and desorbed from external molecules (*e.g.*, oxygen) in water.[35] It can be assumed that the cobalt ions activated PMS to produce $SO_4^{\cdot-}$ and ·OH according to the following equations:[3,36,37]

$$Co^{2+}@NF/ZIF\text{-}67 + HSO_5^- \rightarrow Co^{3+}@NF/ZIF\text{-}67 + SO_4^{\cdot-} + OH^- \quad (1)$$

$$SO_4^{\cdot-} + OH^- \rightarrow \cdot OH + SO_4^{2-} \quad (2)$$

$$Co^{3+}@NF/ZIF\text{-}67 + HSO_5^- \rightarrow Co^{2+}@NF/ZIF\text{-}67 + SO_5^{\cdot-} + H^+ \quad (3)$$

The Co^{2+} ions in ZIF-67 activated HSO_5^- to generate $SO_4^{\cdot-}$; meanwhile, Co^{2+} converted to Co^{3+}, which subsequently activated HSO_5^- to yield $SO_5^{\cdot-}$. The chromophoric groups of RhB could be degraded by the powerful oxidizing potential of $SO_4^{\cdot-}$, leading to decolorization of the dyes. The decolorized dyes might be further degraded to CO_2 and H_2O by $SO_4^{\cdot-}$. Owing to the typical chain reaction, ·OH was also formed during the process, which could contribute to the degradation of RhB.

ESR measurements were performed to detect the radicals probed by DMPO. As shown in Fig. 4A, there were only unclear signals of radicals in the ESR spectrum after adding only PMS. In contrast, significant signals were observed when PMS was added in the system with NF/ZIF-67. The characteristic signals with an intensity ratio of 1 : 2 : 2 : 1 ($\alpha_H = \alpha_H = 14.8$ G) belonged to DMPO–·OH, indicating that ·OH was generated during the PMS activation process. The peaks of DMPO–$SO_4^{\cdot-}$ appeared around the signals of ·OH, providing a direct evidence for the presence of $SO_4^{\cdot-}$ in the system.

To further explain the mechanism of the NF/ZIF-67/PMS system and distinguish the leading role of radicals, free radical capture experiments were performed. According to the literature, methanol is an effective quenching agent of $SO_4^{\cdot-}$, whereas tertiary butyl alcohol (TBA) is usually used as a scavenger for ·OH.[38,39] Moreover, ascorbic acid is often adopted as traps for both ·OH and $SO_4^{\cdot-}$.[40] It can be seen in Fig. 4B that the addition of ascorbic acid significantly inhibited RhB decolorization in the system, implying that the radicals played the major role in RhB degradation. The RhB decolorization rate constant with ascorbic acid (0.013 min^{-1}) was much lower than that of the control experiment without a scavenger (0.285 min^{-1}). Clearly, the addition of TBA in the system led to a relatively high removal efficiency (85.3%) of RhB decolorization, which indicated that ·OH contributed less to the degradation of RhB with NF/ZIF-67-activated PMS. However, the degradation efficiency of RhB significantly reduced to 26.4% when methanol was added in the system, implying that $SO_4^{\cdot-}$ was the exclusive active species for the decolorization of RhB with NF/ZIF-67-activated PMS. The results suggested that both ·OH and $SO_4^{\cdot-}$ were responsible for the decolorization of RhB with NF/ZIF-67-activated PMS. Nevertheless, only a small amount of ·OH was present in the system, which contributed much less compared with $SO_4^{\cdot-}$. Thus, the decolorization of RhB was mainly due to $SO_4^{\cdot-}$ produced during PMS activation by NF/ZIF-67. The proposed heterogeneous activation mechanism is illustrated in Scheme 1.

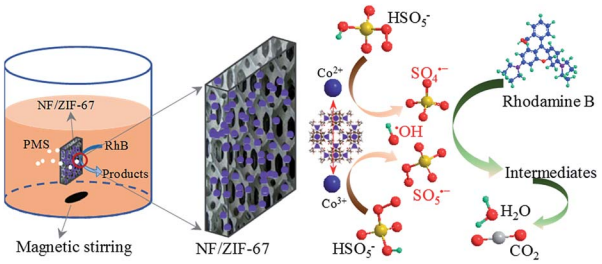

Scheme 1 The proposed mechanism of PMS activation and RhB degradation on NF/ZIF-67.

Recyclability of NF/ZIF-67

The NF/ZIF-67 catalyst has a promising potential for PMS activation and dye decolorization. Recyclability tests of NF/ZIF-67 were carried out for the degradation of RhB. As a macroscopic 3D material, the as-prepared NF/ZIF-67 can be easily separated from the solution, which might simplify operations and increase the recycling efficiency. NF/ZIF-67 retained a high RhB removal efficiency of 90.0% after four cycles of reuse (Fig. 5), which was only 7% lower than that of the first cycle. Moreover, the degradation rate constant of the fourth cycle was 0.132 min^{-1}, indicating that NF/ZIF-67 retained high catalytic activity for PMS activation and RhB degradation. The *in situ* growth of NF/ZIF-67 might closely integrate the ZIF-67 catalyst and NF, leading to less shedding of the catalyst. In addition, the three-dimensional structure of NF/ZIF-67 is beneficial to the transport of reactants and reaction products. Furthermore, NF/ZIF-67 could be easily separated from the solution; thus, further centrifugation or filtration separation processes during the recycle tests could be avoided, resulting in relatively high degradation efficiency after four cycles of reuse. These features indicated that the heterogeneous NF/ZIF-67 catalyst prepared by an *in situ* growth method is a promising recyclable and efficient catalyst for the activation of the oxidant PMS and for organic pollutant degradation.

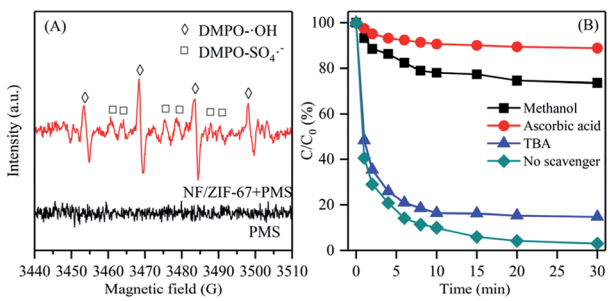

Fig. 4 (A) ESR spectra of NF/ZIF-67-activated PMS with radicals probed by DMPO. (B) Effect of radical scavengers of ascorbic acid, methanol and TBA on the degradation of RhB with NF/ZIF-67-activated PMS. Reaction conditions: RhB concentration of 100 mg L^{-1}, initial pH of 7.0, PMS dosage of 30 mg, and temperature of 25 °C.

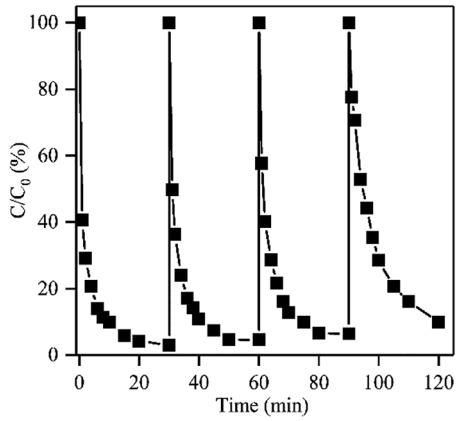

Fig. 5 Four cycles of RhB degradation by NF/ZIF-67-activated PMS. Reaction conditions: RhB concentration of 100 mg L^{-1}, initial pH of 7.0, PMS dosage of 30 mg, and temperature of 25 °C.

Experimental

Materials

Cobalt nitrate hexahydrate, absolute methanol, polyvinyl pyrrolidone (PVP), and rhodamine B were purchased from Kelong Chemical Reagent Co., Ltd (Chengdu, China). 2-Methylimidazolate and peroxymonosulfate (PMS, content: 45 wt%) were supplied by Aladdin Chemical Reagent Co., Ltd (Shanghai, China). The nickel foam was purchased from Lyrun Co., Ltd (Changsha, China). All the solutions were prepared with deionized water obtained with the Milli-Q system. The reagents were used as purchased without further purification.

Preparation of NF/ZIF-67

In this research, nickel foams were tailored into square pieces 3 cm long and 2 mm thick. To clean the surface of the foam and enhance the surface affinity, the square nickel foams were immersed in HCl solution (40 mL, 1 M) containing 0.5 g PVP. After pre-treating for 1 h, the nickel foams were rinsed with deionized water and methanol several times to remove excess PVP. For the direct growth of ZIF-67, the nickel foams were immersed in 100 mL methanol solution with 50 mM $Co(NO_3)_2$ and 50 mM 2-methylimidazole. After growth for 12 h without disturbance, the nickel foams with ZIF-67 were washed with methanol at least three times and dried in a vacuum oven at 80 °C for 12 h. The amount of grown ZIF-67 was determined from the weight of NF before and after ZIF-67 growth, and it was calculated to be 3.7 wt%. The nickel foam with the *in situ* growth of ZIF-67 was labelled as NF/ZIF-67. The morphology and structure of the obtained three-dimensional heterogeneous catalysts were analysed using a scanning electron microscope (SEM, Quanta 250, FEI, US), and the chemical compositions were investigated by energy dispersive spectroscopy (EDS).

Degradation of RhB by NF/ZIF-67-activated PMS

The activation of PMS using NF/ZIF-67 was evaluated by batch-type experiments of RhB dye degradation. In a typical experiment, a piece of NF/ZIF-67 (3 cm × 3 cm) was added into a beaker containing RhB solution (200 mL, 100 mg L^{-1}). NaOH (0.1 M) and HCl (0.1 M) were used to adjust the initial pH value. The solution was stirred for 30 min to adsorb saturated RhB on NF/ZIF-67. Then, a certain dosage of PMS was immediately mixed into the RhB solution, which was stirred continually and maintained at a pre-set temperature (25 °C). Sample aliquots of 1 mL were withdrawn from the solution at regular intervals. Then, 1 mL methanol was immediately mixed into the sample to quench the residual radicals. The residual RhB concentration was determined with a UV-Vis spectrophotometer (Alpha-1500, Shanghai, China) at a maximum wavelength of 554 nm. 5,5-Dimethyl-1-pyrroline *N*-oxide (DMPO, >99 wt%) was utilized to capture the generated hydroxyl and sulfate radicals, which were then detected by electron spin resonance (EMX-10/12, Bruker, Germany). The cobalt ions released in the solution were detected by atomic absorption spectroscopy (AAS, PinAAcle900T, PerkinElmer, US).

Conclusions

In summary, ZIF-67 was successfully grown *in situ* on a nickel foam through a simple method. NF/ZIF-67 was prepared as a 3D heterogeneous catalyst for PMS activation and RhB degradation in an aqueous solution. The factors of PMS dosage and initial concentration of RhB were investigated for RhB degradation. Enhanced RhB degradation was observed using NF/ZIF-67-activated PMS under neutral conditions and high temperatures. Based on the investigations of various radical scavengers, sulfate radicals were the dominant active species compared with hydroxyl radicals for the oxidative decolorization of RhB with NF/ZIF-67-activated PMS. Furthermore, NF/ZIF-67 was confirmed to be a recyclable heterogeneous catalyst for PMS activation with small loss of efficiency after operation for four cycles. Therefore, the simple *in situ* growth method used to prepare NF/ZIF-67 is a promising strategy for constructing heterogeneous catalysts for PMS activation and organic pollutant degradation.

Conflicts of interest

There are no conflicts to declare.

Acknowledgements

The research was supported by the National Natural Science Foundation of China (No. 51708374), the Scientific Research Foundation of Education Department of Sichuan Provincial (No. 18ZA0399) and the Foundation of Key Laboratory of Special Waste Water Treatment, Sichuan Province Higher Education System (No. SWWT2016-1).

References

1 W.-D. Oh, Z. Dong and T.-T. Lim, *Appl. Catal., B*, 2016, **194**, 169–201.
2 F. Ghanbari and M. Moradi, *Chem. Eng. J.*, 2017, **310**, 41–62.

3 P. Hu and M. Long, *Appl. Catal., B*, 2016, **181**, 103–117.
4 M. A. Oturan and J.-J. Aaron, *Crit. Rev. Environ. Sci. Technol.*, 2014, **44**, 2577–2641.
5 G. V. Buxton, C. L. Greenstock, W. P. Helman and A. B. Ross, *J. Phys. Chem. Ref. Data*, 1988, **17**, 513–886.
6 P. Neta, R. E. Huie and A. B. Ross, *J. Phys. Chem. Ref. Data*, 1988, **17**, 1027–1284.
7 S. Verma, S. Nakamura and M. Sillanpää, *Chem. Eng. J.*, 2016, **284**, 122–129.
8 S. Khan, X. He, H. M. Khan, D. Boccelli and D. D. Dionysiou, *J. Photochem. Photobiol., A*, 2016, **316**, 37–43.
9 K.-Y. A. Lin, Y.-C. Chen and Y.-F. Lin, *Chem. Eng. Sci.*, 2017, **160**, 96–105.
10 A. Khan, Z. Liao, Y. Liu, A. Jawad, J. Ifthikar and Z. Chen, *J. Hazard. Mater.*, 2017, **329**, 262–271.
11 Y. Yao, Y. Cai, F. Lu, F. Wei, X. Wang and S. Wang, *J. Hazard. Mater.*, 2014, **270**, 61–70.
12 C. Cai, H. Zhang, X. Zhong and L. Hou, *J. Hazard. Mater.*, 2015, **283**, 70–79.
13 P. Shukla, H. Sun, S. Wang, H. M. Ang and M. O. Tadé, *Catal. Today*, 2011, **175**, 380–385.
14 P. Shi, R. Su, F. Wan, M. Zhu, D. Li and S. Xu, *Appl. Catal., B*, 2012, **123**, 265–272.
15 S. Kitagawa, *Chem. Soc. Rev.*, 2014, **43**, 5415–5418.
16 H. Furukawa, K. E. Cordova, M. O'Keeffe and O. M. Yaghi, *Science*, 2013, **341**, 1230444.
17 J. A. Mason, M. Veenstra and J. R. Long, *Chem. Sci.*, 2014, **5**, 32–51.
18 S. You, X. Gong, W. Wang, D. Qi, X. Wang, X. Chen and N. Ren, *Adv. Energy Mater.*, 2016, **6**, 1501497.
19 Y. Jian, Z. Fengjun, L. Haiyuan, H. Xun, J. Hailong, W. Yuen and L. Yadong, *Angew. Chem., Int. Ed.*, 2015, **54**, 10889–10893.
20 N. A. Khan, B. K. Jung, Z. Hasan and S. H. Jhung, *J. Hazard. Mater.*, 2015, **282**, 194–200.
21 C.-C. Wang, J.-R. Li, X.-L. Lv, Y.-Q. Zhang and G. Guo, *Energy Environ. Sci.*, 2014, **7**, 2831–2867.
22 N. A. Khan, Z. Hasan and S. H. Jhung, *J. Hazard. Mater.*, 2013, **244**, 444–456.
23 W. Ma, Y. Du, N. Wang and P. Miao, *Environ. Sci. Pollut. Res.*, 2017, **24**, 16276–16288.
24 K.-Y. A. Lin and H.-A. Chang, *J. Taiwan Inst. Chem. Eng.*, 2015, **53**, 40–45.
25 J.-y. Pu, J.-q. Wan, Y. Wang and Y.-w. Ma, *RSC Adv.*, 2016, **6**, 91791–91797.
26 T. Shen, Q. Wang and S. Tong, *Ind. Eng. Chem. Res.*, 2017, **56**, 10965–10971.
27 F. Dong, Z. Wang, Y. Li, W.-K. Ho and S. Lee, *Environ. Sci. Technol.*, 2014, **48**, 10345–10353.
28 P. Shao, X. Duan, J. Xu, J. Tian, W. Shi, S. Gao, M. Xu, F. Cui and S. Wang, *J. Hazard. Mater.*, 2017, **322**, 532–539.
29 J. Zhao, T. Wu, K. Wu, K. Oikawa, H. Hidaka and N. Serpone, *Environ. Sci. Technol.*, 1998, **32**, 2394–2400.
30 F. Ji, C. Li and L. Deng, *Chem. Eng. J.*, 2011, **178**, 239–243.
31 A. Rastogi, S. R. Al-Abed and D. D. Dionysiou, *Appl. Catal., B*, 2009, **85**, 171–179.
32 F. Qi, W. Chu and B. Xu, *Chem. Eng. J.*, 2014, **235**, 10–18.
33 K.-Y. A. Lin, H.-A. Chang and R.-C. Chen, *Chemosphere*, 2015, **130**, 66–72.
34 J. Lu, Q. Liu, Z. Xiong, Z. Xu, Y. Cai and Q. Wang, *J. Chem. Technol. Biotechnol.*, 2017, **92**, 1601–1612.
35 G. Saracco, S. Vankova, C. Pagliano, B. Bonelli and E. Garrone, *Phys. Chem. Chem. Phys.*, 2014, **16**, 6139–6145.
36 R. Luo, C. Liu, J. Li, J. Wang, X. Hu, X. Sun, J. Shen, W. Han and L. Wang, *J. Hazard. Mater.*, 2017, **329**, 92–101.
37 K.-Y. A. Lin and B.-J. Chen, *Chemosphere*, 2017, **166**, 146–156.
38 X. Li, W. Guo, Z. Liu, R. Wang and H. Liu, *Appl. Surf. Sci.*, 2016, **369**, 130–136.
39 M. E. Lindsey and M. A. Tarr, *Environ. Sci. Technol.*, 2000, **34**, 444–449.
40 Z. Huang, H. Bao, Y. Yao, W. Lu and W. Chen, *Appl. Catal., B*, 2014, **154**, 36–43.